Dimension Variation Prediction for Composites

Chensong Dong, Chuck Zhang*, Zhiyong Liang and Ben Wang

Department of Industrial Engineering
Florida A&M University – Florida State University
Tallahassee, FL 32310, USA

* Corresponding Author

June 18, 2003

Abstract

This paper presents an innovative study on the dimension variation prediction and control for polymer matrix fiber reinforced composites. A dimension variation model was developed for process simulation based on thermal stress analysis and finite element analysis (FEA). This model was validated against the experimental data, the analytical solutions and the data from literature. Using the FEA-based dimension variation model, the deformations of typical composite structures were studied and the regression-based dimension variation model was developed. By introducing the material modification coefficient, this comprehensive model can account for various fiber/resin types and stacking sequences. The regression-based dimension variation model can significantly reduce computation time by eliminating the complicated, time-consuming finite element meshing and material parameter defining process, which provides a quick design guide for composite products with reduced dimension variations. The structural tree method (STM) was developed to compute the assembly deformation from the deformations of individual components, as well as the deformation of general shape composite components. The STM enables rapid dimension variation analysis/synthesis for complex composite assemblies with the regression-based dimension variation model. The exploring work presented in this research provides a foundation to develop practical and proactive dimension control techniques for composite products.

Introduction

The last four decades have seen a tremendous advancement in the science and technology of fiber-reinforced composites. The low density, high strength, high stiffness to weight ratio, excellent durability, and design flexibility of composites are the primary reasons for their use in many structural components in aircraft, automotive, marine, and other industries [1]. One of the obstacles for composite applications is the dimension infidelity. Traditional dimension control operations for composites are mainly based on trial-and-error approaches, which cannot be directly and effectively employed in real world part design and tooling development. In another aspect, the increasing applications of new processes, such as resin transfer molding (RTM) and vacuum assisted resin transfer molding (VARTM), will also raise a number of new issues in dimension control. For example, large warpage in RTM process is observed due to the occurrences of resin rich surfaces and resin rich zones [2]. With the increasing requirement for composite products to be affordable, net-shaped, and assembly efficient, effective dimension control is highly desirable.

The dimension variations of composites have been studied experimentally [3-5], analytically [6-13] and numerically [14-22].

Spring-in is a common problem in composite fabrication caused by the difference between the in-plane thermal expansion coefficient and the through-thickness thermal expansion coefficient. For simple geometric structures as “L-shaped,” the spring-in has been analytically computed for the autoclave process [6-10], the RTM process [6-9] and the filament winding process [11-13].

In order to predict the spring-in of more complex structures, numerical simulation tools of finite element method or finite difference method have been employed. Theriault et al. [14]

developed a one-dimensional finite difference model to simulate the progression of material properties during the processing of metal-clad, multi-layered, fiber mat reinforced, thermoset resins. The general Classical Lamination Theory was implemented to evaluate the dimensional movement of the composite laminate. Wiersma et al. [15] predicted the spring-in using the finite element method. Curing simulation, elastic model and viscoelastic model were studied. Darrow and Smith [16-17] employed the finite element method to model the processing induced spring-in in laminated composites. Their model accounted for the mold stretching, thickness shrinkage, and fiber volume fraction gradients, which was able to account for 80% of the observed spring-in for parts ranging between 1 and 5 mm thick and having a 3 to 13 mm bend radius. Golestanian and El-Gizawy [18] modeled the process-induced residual stresses and deformation in composite parts using the finite element method coupled with cure-dependent mechanical properties. Wang et al. [19] conducted a finite element analysis of spring-in using ABAQUS. Fernlund et al. [20] presented an engineering approach to predict process-induced deformations of three-dimensional composite shell structures, using a two-dimensional special purpose finite element process code COMPRO and a standard three-dimensional structural code ANSYS.

A number of full 3-D spring-in models have been developed recently. Ding et al. [21] developed a 3-D finite element analysis procedure to predict “spring-in” resulting from anisotropy for both thin and thick angled composite shell structures. Zhu et al. [22] developed a fully 3-D coupled thermo-chemo-viscoelastic finite element model to simulate the heat transfer, curing, and residual stress development during the manufacturing cycle of thermoset composite parts.

From the literature review, it is seen that many studies have focused on the curing process and residual stresses in composite processing. Various models were proposed for the deformation prediction of composite structures. However, most of them were based on finite element analysis and they are not convenient for industry applications. The influence of design on the dimension variations has not been fully investigated, which is necessary to achieve good dimension control in the early design stage. In addition, the prediction and control for deformations of composite assemblies lack a thorough study. Thus, it is highly desirable to develop an engineering tool for composite component and assembly design with good dimension control.

In this study, a regression-based dimension variation model was developed based on the study of typical composite structures using the FEA-based dimension variation model. The structural tree method (STM) was developed to compute the deformations of general shape composite components and composite assemblies. Using the regression-based dimension variation model and the structural tree method, the dimension variations of composite products and assemblies can be predicted effectively and efficiently.

2 Research Methodology

The research methodology is illustrated in Figure 1, which includes dimension variation model development and validation, typical structure study, regression analysis, deformation compensation, and design optimization and tolerance analysis/synthesis for composite assemblies.

First, a dimension variation model was developed based on thermal stress analysis and FEA. The deformation of composites can be computed using the developed dimension variation model. However, this approach is FEA-based. The FEA for composite modeling involves a

complicated geometric modeling and meshing process, as well as a large amount of parameter input work due to the layer-wise structure of composites. This requires extensive FEA knowledge and skills for users. The computation is often time-consuming when the geometry becomes complex and the number of nodes and elements becomes large. All of these limit its applications in industry. Thus, typical composite structures were investigated and the influences of design parameters on the deformation were studied. The regression-based dimension variation model was developed.

The deformations of typical composite structures can be computed using the regression-based dimension variation model. However, it cannot be directly used to compute the deformation of general shape composite parts and composite assemblies. Thus, a method called the structural tree method based on coordinate transformation was developed since the deformations of typical composite structures are mostly angular ones.

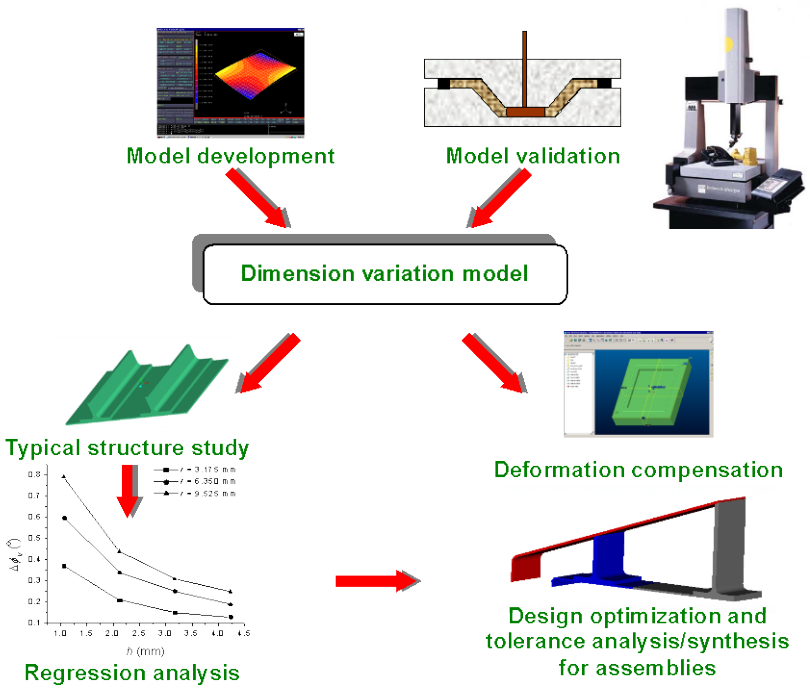

Figure 1: Research methodology

3 Dimension Variation Model

3.1 FEA-Based Dimension Variation Model

In order to predict the dimension variations of composite products, a dimension variation model was first developed based on thermal stress analysis and finite element analysis (FEA) in this research. The procedure is shown in Figure 2. A non-isothermal flow and curing model was first utilized to simulate the flow pattern and temperature distribution. A material model was used to compute the material properties, i.e. CTE, moduli, etc. These results, with the design geometry and processing parameters, were imported into the dimension variation model, which was based on the Classic Lamination Theory (CLT) and FEA, to compute the deformation. Using the same design geometry, material properties and processing parameters, experimental parts were fabricated and measured using a coordinate measuring machine. The experimental data, as well as the analytical solutions and the data from literature, were used to illustrate the effectiveness of the FEA-based dimension variation model.

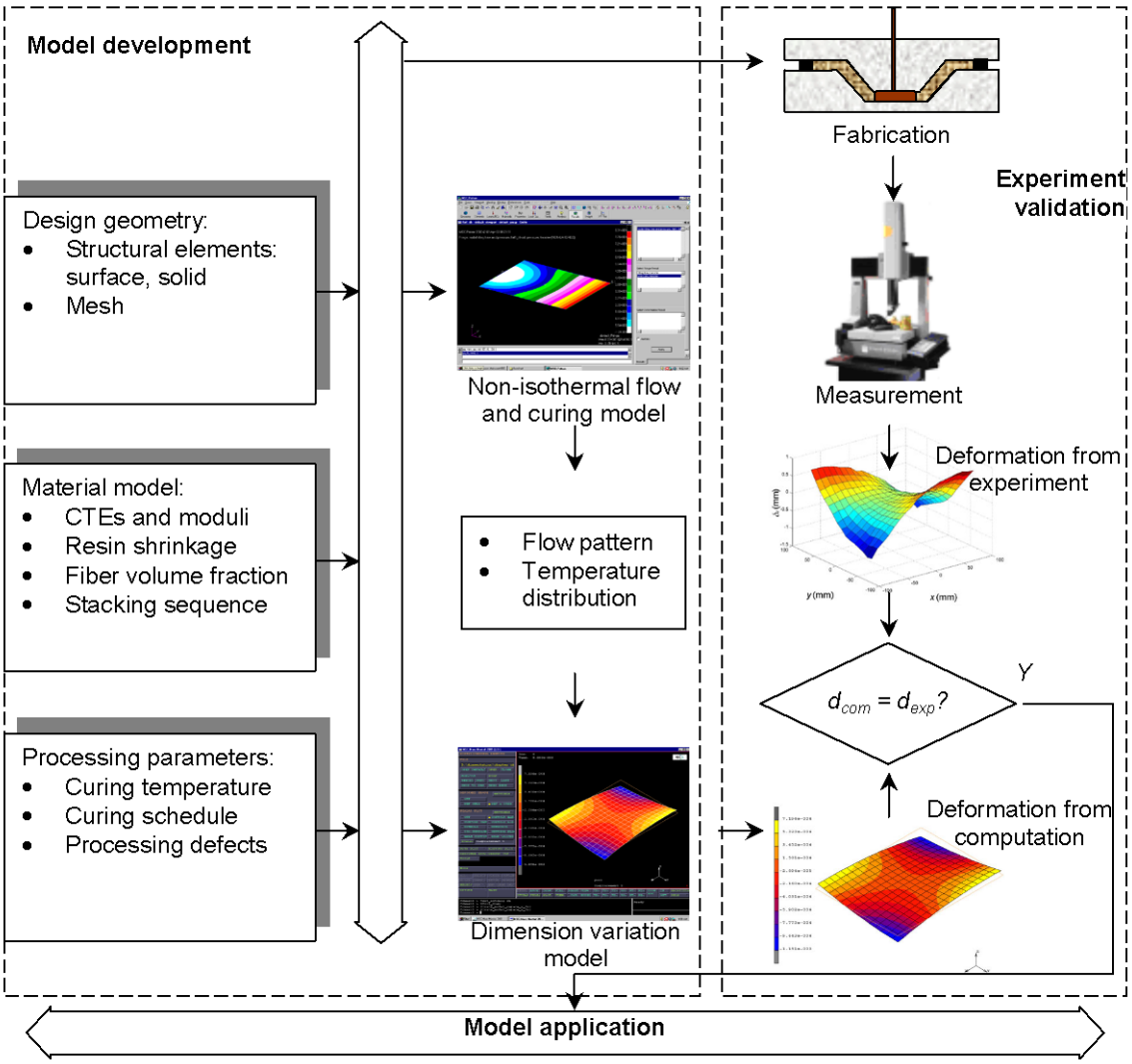

Figure 2: Dimension variation model development and validation

3.1.1 Material Model

Elastic properties of a unidirectional lamina are calculated from the following equations [23]:

$$E_{11} = E_f V_f + E_m V_m \tag{1}$$

$$\nu_{12} = \nu_f V_f + \nu_m V_m \tag{2}$$

$$E_{22} = \frac{(V_f + \eta_{22} V_m) E_f E_m}{(V_f E_m + \eta_{22} V_m E_f)} \tag{3}$$

$$G_{12} = \frac{(V_f + \eta_{12} V_m) G_f G_m}{(V_f G_m + \eta_{12} V_m G_f)} \tag{4}$$

where:

V_f: fiber volume fraction

E_f, E_m: elastic modulus of fiber and matrix, respectively

G_f, G_m: shear modulus of fiber and matrix, respectively

v_f, v_m: Poisson's ratio of fiber and matrix, respectively

E_{11}: longitudinal modulus of 0° fiber lamina

E_{22}: transverse modulus of 0° fiber lamina

G_{12}: shear modulus of 0° fiber lamina

η_{22}, η_{12}: stress-partitioning parameters

For epoxy matrix composites, η_{22} and η_{12} are shown in Table 1.

Table 1: Stress-partitioning parameters

	Fiber Type		
	Carbon	Glass	Kevlar-49
η_{22}	0.5	0.516	0.516
η_{12}	0.4	0.516	0.4

When expanded to 3-D, the mechanical properties can be obtained as [24]:

$$E_{33} = E_{22} \tag{5}$$

$$\nu_{13} = \nu_{12} \tag{6}$$

$$\nu_{23} = \nu_{32} = 1 - \nu_{21} - \frac{E_{22}}{3K} \tag{7}$$

$$G_{13} = G_{12} \tag{8}$$

$$G_{23} = G_{32} = \frac{E_{22}}{2(1+\nu_{23})} \tag{9}$$

where K is the bulk modulus of the composite.

For a unidirectional continuous fiber lamina, coefficients of linear thermal expansion in the 0 and 90º directions can be calculated from the following equations:

$$\alpha_{11} = \frac{\alpha_{fl} E_f V_f + \alpha_m E_m V_m}{E_f V_f + E_m V_m} \tag{10}$$

and

$$\alpha_{22} = (1+\nu_f)\frac{\alpha_{fl} + \alpha_{fr}}{2} V_f + (1+\nu_m)\alpha_m V_m - \alpha_{11}\nu_{12} \tag{11}$$

where

α_{fl}: coefficient of linear thermal expansion for the fiber in the longitudinal direction

α_{fr}: coefficient of linear thermal expansion for the fiber in the radial direction

α_m: coefficient of linear thermal expansion for the matrix

If the fibers are at an angle θ with x direction, the coefficients of thermal expansion in the x and y directions can be calculated using α_{11} and α_{22}:

$$\alpha_{xx} = \alpha_{11}\cos^2\theta + \alpha_{22}\sin^2\theta \tag{12a}$$

$$\alpha_{yy} = \alpha_{11}\sin^2\theta + \alpha_{22}\cos^2\theta \tag{12b}$$

$$2\alpha_{xy} = 2(\alpha_{11} - \alpha_{22})\sin\theta\cos\theta \tag{12c}$$

where α_{xx} and α_{yy} are coefficients of linear expansion and α_{xy} is the coefficient of shear expansion. When expanded to 3-D,

$$\alpha_{yz} = \alpha_{zx} = 0 \tag{13}$$

$$\alpha_{zz} = \alpha_{33}. \tag{14}$$

Curing shrinkage occurs because of the rearrangement of polymer molecules into a more compact mass as the curing reaction proceeds. A volumetric shrinkage of 1-5% has been found for epoxies [1]. Considering the modulus change in curing, a lower bound value of curing shrinkage 1% was assumed for epoxy. The concept of equivalent CTE [16-17] was introduced to account for the resin shrinkage during the curing process. By converting the curing shrinkage to the form of the CTE, the effects of CTE mismatch and curing shrinkage can be modeled simultaneously. The curing shrinkage can be expressed as V_s. The volumetric change of resin is $1 + V_s$. This can be regarded as the following equation after neglecting the high order items.

$$\left[1+V_s/(3\Delta T)\right]^3 = 1+3V_s/(3\Delta T)+3\left[V_s/(3\Delta T)\right]^2+\left[V_s/(3\Delta T)\right]^3. \tag{15}$$

The equivalent CTE of resin can be expressed as:

$$\alpha_r^e = \alpha_r + V_s/(3\Delta T) \tag{16}$$

where,

α_r^e: equivalent CTE of epoxy

α_r: CTE of epoxy

V_s: shrinkage of resin.

3.1.2 FEA-based Dimension Variation Model Validation

The FEA-based dimension variation model was validated against the analytical solutions and experimental data. First, the model was validated against the analytical solutions and experimental data in [8-9]. An L-shaped structure was made from carbon fiber and epoxy. The deformation was due to the CTE mismatch in the in-plane direction (α_I) and the through-thickness direction (α_T), which is commonly called “spring-in,” as shown in Figure 3.

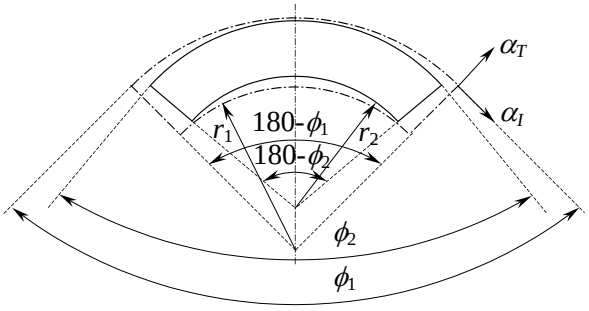

Figure 3: Spring-in of an L-shaped structure

The fiber volume fraction is about 50.3% and the processing temperature is 160°C. Several laminates of various stack sequence, inner radius of the tool, and thickness were investigated using the FEA-based dimension variation model. The results are compared with the analytical solutions and experimental data in Table 2.

Table 2: Comparison among computational results, analytical solutions and experimental results for the L-shaped carbon/epoxy parts

Stacking sequence	Internal radius r_i (mm)	Computational result (°) in this study	Experimental result (°) [8-9]	Theoretical result (°) [8-9]
$[0]_4$	3.0	-1.69	-0.99	-1.72
$[0]_4$	6.0	-1.69	-2.34	-1.72
$[0]_8$	6.0	-1.70	-1.70	-1.72
$[-45/45]_s$	3.0	-1.47	-1.66	-1.69
$[-45/45]_s$	6.0	-1.51	-1.37	-1.69
$[-45/-45/45/45]_s$	6.0	-1.52	-1.59	-1.69
$[90]_4$	3.0	-1.29	-1.81	-1.30
$[90]_4$	6.0	-1.29	-0.91	-1.30
$[90]_8$	6.0	-1.30	-0.76	-1.30

It is shown that the FEA results agree well with the analytical solutions. Considering the fact that the spring-in is independent to the radius and thickness, the spring-in values were averaged for each stacking sequence and plotted in Figure 4. It is seen that on the average, the

experimental results agree well with the FEA results. However, the experimental results scatter significantly, possibly caused by the processing defects, such as resin rich zone due to resin flow.

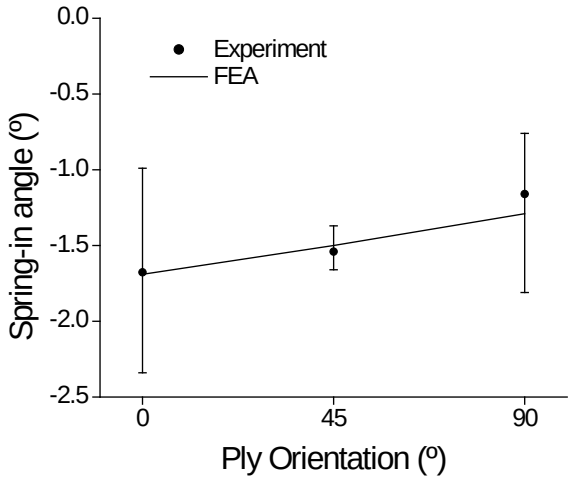

Figure 4: Comparison between computational results and experimental results for the L-shaped carbon/epoxy parts

Secondly, a single-stiffener structure was modeled, fabricated, and measured to validate the FEA-based dimension variation model. The mold assembly is shown in Figure 5. The parts were made from E-glass fiber mats and epoxy resin. The unidirectional fiber mats (Cofab A1010) were cut to fit the mold cavity. The epoxy resin used was Shell Epon® Resin 862. It was mixed with EPI-CURE® W Curing Agent at the ratio of 100:26.4 by weight. The mixed resin system was heated to decrease the viscosity. The assembled mold was preheated to 100°C. The resin was injected into the mold cavity at a constant pressure 0.1 MPa. After the mold filling process, the mold was cured at 177°C for two hours. After cool-down the part was demolded. One finished part is shown in Figure 6. The fiber volume fraction was determined experimentally as 22%. The thickness of the part was measured using a caliper at several

positions. Since the thickness change due to processing is less than 0.2 μm, the actual part thickness values were used to build the geometric model.

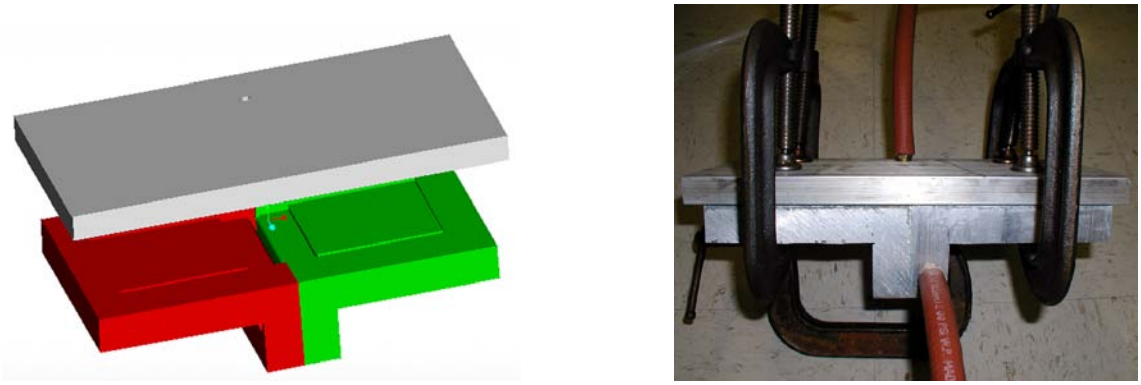

Figure 5: Mold assembly for the single-stiffener structure

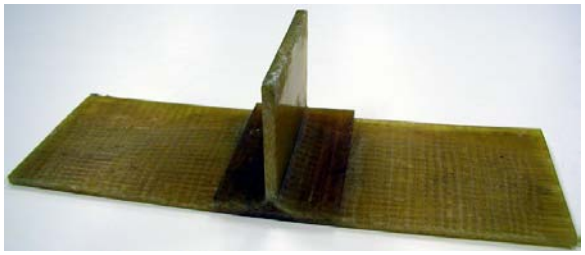

Figure 6: A finished single-stiffener part

After the fiber volume fraction and the thickness were determined, the FEA was conducted. Because of the limited skills for laying up the fiber mats, resin rich zones are formed in the center and on the surface of the part, as shown in Figure 7. These resin rich zones had a significant influence on deformation, and were included in FEA modeling by defining some elements as pure resin. Half of the structure was modeled because of the symmetry. Two stacking sequences $[0/90]_s$ and $[90]_4$ were studied. The computational results are shown in

Figure 8, where the contour shows the total displacement in mm. The spring-in angle of $[0/90]_s$ laminates is -0.49° and that of $[90]_4$ laminates is -0.06°.

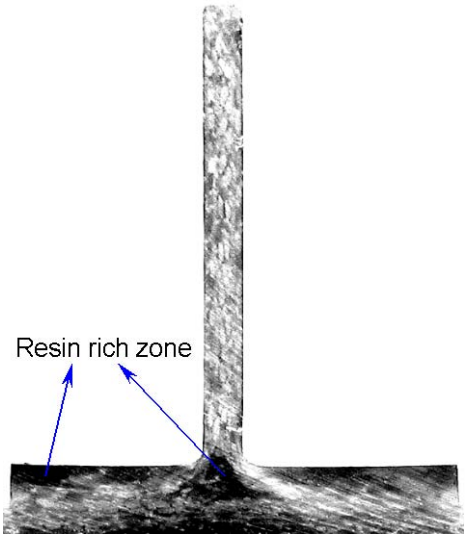

Figure 7: Resin rich zones

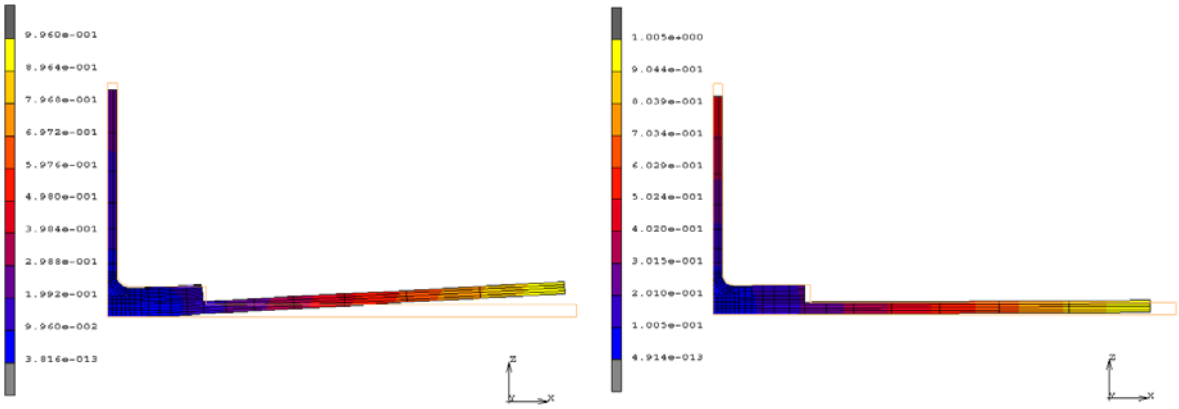

(a): Deformation of $[0/90]_s$ laminates (b): Deformation of $[90]_4$ laminates

Figure 8: FEA result for the single-stiffener structure

The fabricated parts were measured using a CMM, as shown in Figure 9. The results were compared with the computational results as shown in Table 3. Both cases shown that the experimental data agree with the computational results.

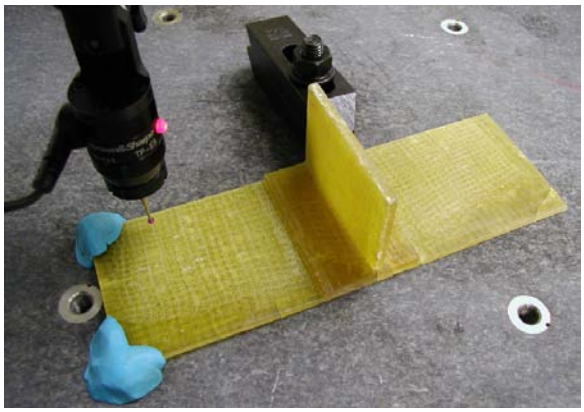

Figure 9: Spring-in measurement of the single-stiffener part

Table 3: Comparison between computational results and experimental results for the single-stiffener E-glass/epoxy parts

	Computational result (°)	Experimental result (°)	Relative error
$[0/90]_s$	-0.49	-0.52	6%
$[90]_4$	-0.063	-0.080	20%

3.2 Regression-Based Dimension Variation Model

3.2.1 Model Development

The deformation of composites is determined by design geometric parameters, material parameters and processing parameters. This gives us a functional relationship as

$$\boldsymbol{\delta} = f(G, M, P) \tag{17}$$

where

$\boldsymbol{\delta}$: deformation vector

G: design geometric parameters

M: material parameters (fiber, resin)

P: processing parameters (temperature, curing)

Since geometry is one of the primary factors determining the deformation of composites, research attention can be focused onto several typical structures such as angled structures, stiffener structures, etc. The purpose is to relate their deformations with the structural parameters and develop a regression-based dimension variation model.

First, the materials were fixed (E-glass/epoxy) in order to study the effects of geometric parameters. Based on experience, seven commonly used typical structures were chosen, as shown in Table 4, together with their corresponding tolerances and design parameters. The developed dimension variation model was used to simulate the deformation of composites. Data were collected by modifying the geometric parameters such as radius and thickness. Non-linear regression models were developed based on these collected data.

Table 4: Typical structures and design parameters

Typical structure	Tolerances	Design parameters
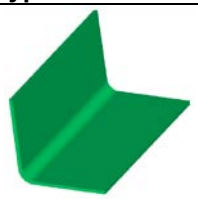 Angled structure	Perpendicularity Angularity	Angle ϕ Radius *r* Thickness *h*
 Single-stiffener structure	Perpendicularity	Radius *r* Thickness *h*
 Multiple-stiffener structure	Perpendicularity Parallelism	Radius *r* Thickness *h*
 Cylindrical shell	Cylindricity	Radius *r* Thickness *h*
 Hat-shaped structure	Flatness	Radius *R*, *r* Thickness *h*
 Structure with an open window	Flatness	Size Stiffener thickness *t* Thickness *h*
 3-D stiffener structure	Flatness	Size Stiffener thickness *t* Thickness *h*

A single-stiffener structure was used to illustrate the approach. The spring-in of the single-stiffener structure is controlled by the perpendicularity. With reference to Figure 10, the

design parameters possibly affecting the perpendicularity are the half-length $L/2$, the height H, the inner radius r, and the thickness h. The perpendicularity is proportional to the half-length of the structure, $L/2$. Thus, the spring-in angle was investigated alternatively to reduce the number of design parameters. It is related to the perpendicularity as

$$T_{pe} = L\Delta\phi/2 \tag{18}$$

where T_{pe} is the perpendicularity; $L/2$ is the half-length of the single-stiffener structure; and $\Delta\phi$ is the spring-in angle.

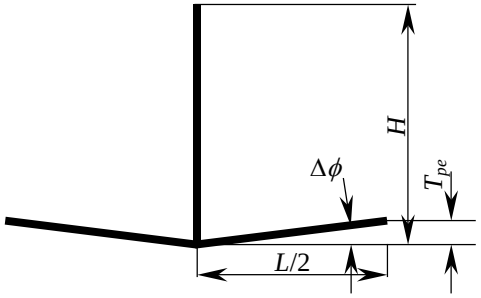

Figure 10: Tolerances of the single-stiffener structure

The cross ply E-glass/epoxy laminates were first studied. First, the fiber volume fraction was fixed at 49%. The design parameters and levels are shown in Table 5.

Table 5: Design parameters and levels for single-stiffener structures

Thickness h (mm)	Radius r (mm)	Fiber volume fraction V_f
1.058	3.175	0.41
2.117	6.35	0.49
3.175	9.525	0.57
4.233	—	0.66

The spring-in was simulated using the FEA-based dimension variation model. The results are shown in Figure 11. The spring-in angle increases linearly with the increase of inner

radius *r* and decreases exponentially with the increase of thickness *h*. This is because of the existence of resin rich zones. The resin shrinks much more than the lamina, and its modulus is much lower than that of the lamina.

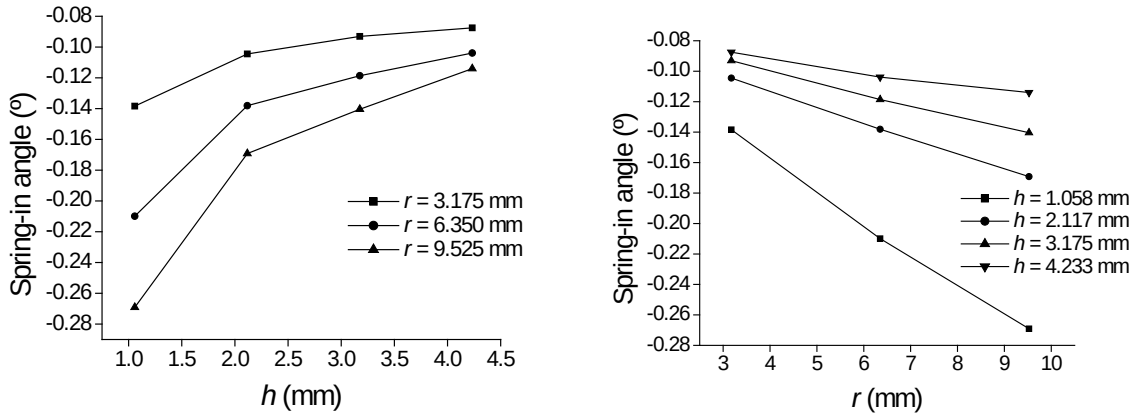

(a) Spring-in vs. thickness *h* (b) Spring-in vs. radius *r*

Figure 11: Influences of radius and thickness on the spring-in of single-stiffener structures

In addition, the effect of fiber volume fraction was also studied. The results are shown in Figure 12. The spring-in angle decreases with the increase of the fiber volume fraction.

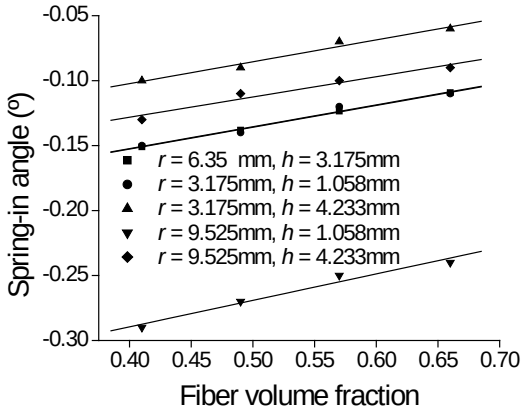

Figure 12: Influence of fiber volume fraction on the spring-in of single-stiffener structures

Similarly, in order to reveal the effects of the stacking sequence, the spring-in of symmetric angle ply laminates was investigated. In the study cases, the inner radius is 3.175 mm, 6.35 mm, and 9.525 mm, respectively; and the thickness is 2.117 mm. The results are shown in Figure 13. When the fiber orientation changes from 0 to 90°, the difference between the in-plane CTE and the through-thickness CTE decreases, thus the spring-in angle decreases.

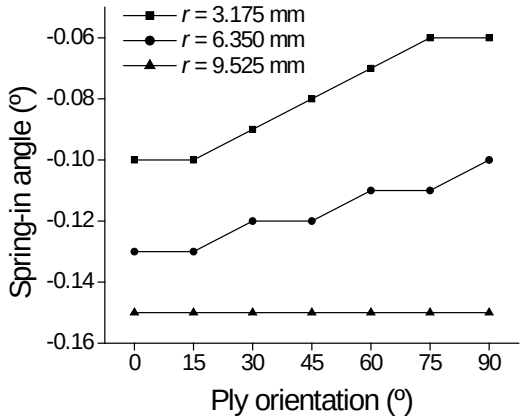

Figure 13: Spring-in of angle ply E-glass/epoxy laminates $[\theta/\text{-}\theta]_{ns}$

By examining the curves of $\Delta\phi$ vs. r, linear relationships exhibit. Thus, linear regression models were developed as follows for h = 1.058 mm to 4.233 mm, respectively.

$$\Delta\phi = -0.075 - 0.021r, \qquad (h = 1.058 \text{ mm}) \tag{19a}$$

$$\Delta\phi = -0.073 - 0.010r, \qquad (h = 2.117 \text{ mm}) \tag{19b}$$

$$\Delta\phi = -0.070 - 0.007r, \qquad (h = 3.175 \text{ mm}) \tag{19c}$$

$$\Delta\phi = -0.075 - 0.004r. \qquad (h = 4.233 \text{ mm}) \tag{19d}$$

Equation 19 shows that the constant term is nearly constant for the four cases. When examining the slope, an exponential decay relationship exhibits. Thus, the slopes can be regressed using an exponential decay model. The regression model for V_f = 49% is

$$\Delta\phi = -0.073 - \left(0.003 + 0.040e^{-\frac{h}{1.264}}\right)r. \tag{20}$$

By examining the curves of $\Delta\phi$ vs. fiber volume fraction, linear relationships exist and the slopes are nearly the same. Thus the final regression model for the spring-in of E-glass/epoxy single-stiffener structures is

$$\Delta\phi = -0.073 - \left(0.003 + 0.040e^{-\frac{h}{1.264}}\right)r + 0.173\left(V_f - 0.49\right). \tag{21}$$

The fitted values and original values are compared in Figure 14. The relative errors are within ±7%.

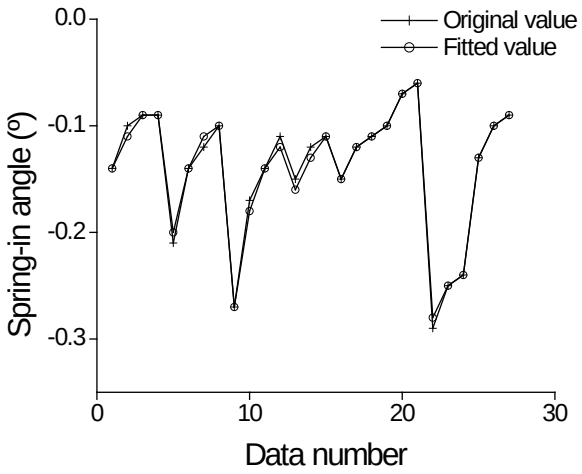

Figure 14: Comparison between fitted values and original values of spring-in for single-stiffener structures

If the resin rich zone is filled with fiber, a decrease in the spring-in is observed, as shown in Figure 15, where r = 6.35 mm and V_f = 49%.

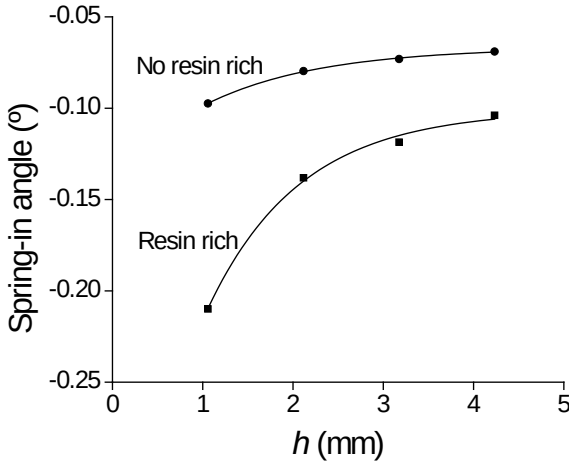

Figure 15: Influence of filling the resin rich zone with fibers on the spring-in

In the same approach, the regression model for E-glass/epoxy single-stiffener structures without resin rich is

$$\Delta\phi = -0.058 - 0.001\left(- 0.783 + 10.806e^{-\frac{h}{2.439}} \right) r + 0.198\left(V_f - 0.49\right). \tag{22}$$

3.2.2 Material Modification Coefficient

In order to obtain a comprehensive model, which is suitable for other materials, a material modification coefficient was introduced, based on the analytical solutions and FEA data. By incorporating this coefficient, the models can be used for any fiber/resin type and any stacking sequence.

For structures including angled structures, cylindrical shells, hat-shaped structures, structures with an open window, or 3-D stiffener structures, the material modification coefficient can be estimated as

$$C_1 = \frac{\left(\alpha_T - \alpha_I\right)\Delta T / \left(1 + \alpha_T \Delta T\right)}{\left(\alpha_{T0} - \alpha_{I0}\right)\Delta T_0 / \left(1 + \alpha_{T0} \Delta T_0\right)}. \tag{23}$$

where

α_I: in-plane CTE

α_T: through-thickness CTE

α_{I0}: reference in-plane CTE (E-glass/epoxy cross ply laminates)

α_{T0}: reference through-thickness CTE (E-glass/epoxy cross ply laminates)

α_{I0} and α_{T0} are solved as follows:

$$\alpha_{I0} = \frac{\alpha_{xx,0} E_{xx,0} + \alpha_{xx,90} E_{xx,90}}{E_{xx,0} + E_{xx,90}} = \frac{\alpha_{11} E_{11} + \alpha_{22} E_{22}}{E_{11} + E_{22}} \tag{24a}$$

$$\alpha_{T0} = \alpha_{zz} = \alpha_{33} \tag{24b}$$

For a general laminate [$\theta_1/\theta_2/\ldots/\theta_{n-1}/\theta_n$], the α_I and α_T are solved as follows:

$$\alpha_I = \frac{\sum_{i=1}^{n} \alpha_{xx,\theta_i} E_{xx,\theta_i}}{\sum_{i=1}^{n} E_{xx,\theta_i}} \tag{25a}$$

$$\alpha_T = \alpha_{zz} = \alpha_{33} \tag{25b}$$

For an angle ply symmetric laminate $[\theta/\text{-}\theta]_{ns}$, the α_I and α_T are solved as follows:

$$\alpha_I = \frac{\alpha_{xx,\theta} E_{xx,\theta} + \alpha_{xx,-\theta} E_{xx,-\theta}}{E_{xx,\theta} + E_{xx,-\theta}} \tag{26a}$$

$$\alpha_T = \alpha_{zz} = \alpha_{33} \tag{26b}$$

For single-stiffener and double-stiffener structures, the coefficients can be estimated as

$$C_2 = \frac{\alpha_m \Delta T / (1 + \alpha_m \Delta T)}{\alpha_{m0} \Delta T_0 / (1 + \alpha_{m0} \Delta T_0)}. \tag{27}$$

where

α_m: CTE of matrix

α_{m0}: reference CTE (CTE of epoxy)

ΔT: temperature change

ΔT_0: reference temperature change (E-glass/epoxy cross ply laminates, 168°C)

The comprehensive regression models for any fiber/resin system and any stacking sequence are summarized in Table 6.

Table 6: Regression models for typical composite structures

Angled structures

$$\Delta\phi = C_1\left(-0.826 + 0.951V_f\right)\left(180 - \phi\right)/90$$

Single-stiffener structures

With resin rich:

$$\Delta\phi = C_2\left[-0.073 - \left(0.003 + 0.040e^{-\frac{h}{1.264}}\right)r + 0.173\left(V_f - 0.49\right)\right]$$

Without resin rich:

$$\Delta\phi = C_2\left[-0.058 - 0.001\left(-0.783 + 10.806e^{-\frac{h}{2.439}}\right)r + 0.198\left(V_f - 0.49\right)\right]$$

Double-stiffener structures

With resin rich:

$$\Delta\phi_v = C_2\left[0.066 + 0.3e^{-\frac{h}{0.971}} + \left(0.016 + 0.121e^{-\frac{h}{1.207}}\right)r - 0.561\left(V_f - 0.49\right)\right]$$

Without resin rich:

$$\Delta\phi_v = C_2\left[0.026 + 0.817e^{-\frac{h}{0.510}} + \left(-0.046 + 0.097e^{-\frac{h}{10.718}}\right)r - 0.637\left(V_f - 0.49\right)\right]$$

Cylindrical shells

$$T_{cy} = 0.006C_1\left[\phi/180 + \left(\phi/180\right)^2\right]\left(1 - V_f\right)r$$

Hat-shaped structures

$$\Delta\phi = C_1\left[-0.694 + 0.8V_f + \left(0.389 - 0.45V_f\right)\exp\left(-R/49.29\right)\right]$$

Structures with an open window

$$\delta_z/a = C_1\sqrt{\frac{a}{200}}0.001\left[1 - 2.468\left(V_f - 0.49\right)\right]\left[5.210 - \left(4.916 + 6.972e^{-\frac{h}{2.585}}\right)e^{-\frac{100t}{\left(-2.409+1.294h\right)a}}\right]$$

3-D stiffener structures

$$\delta_z/a = C_1\sqrt{\frac{a}{400}}0.001\left[1 - 2.325\left(V_f - 0.49\right)\right]\left[\left(3.900 + 0.483h\right) - \left(5.617 + 0.253h\right)e^{-\frac{100t}{\left(-4.792+1.919h\right)a}}\right]$$

The advantage of the non-linear regression-based dimension variation model is that it does not require FEA, thus significantly reduces the amount of computation time. Furthermore, the regression-based dimension variation model provides a quick guide for composite product design with reduced dimension variations.

4 Structural Tree Method

The deformations of typical composite structures can be computed using the regression-based dimension variation model. It is desirable to obtain the deformation of general shape composite parts and composite assemblies. Because the deformations of typical composite structures are mostly angular ones, a method called the structural tree method based on coordinate transformation was developed. The procedure of the STM is as follows:

1. For a given composite assembly, from the origin, identify typical structures, e.g. angled structures, single-stiffener structures…
2. Assign deformation feature points $\mathbf{N_1}$…$\mathbf{N_n}$ based on typical structure study. Generally, these points are assigned at the curved sections of these structures.
3. Construct a structural tree based on these points; each point will form a node of the tree

   $\mathbf{N_0} \longrightarrow \mathbf{N_1} \longrightarrow \cdots \longrightarrow \mathbf{N_n}$.

4. Using the regression models, determine the rotational angle ε_i of node i with reference to its prior node along the path; Formulate the conversion matrix $\mathbf{R_{NiNi\text{-}1}}$ as

$$\mathbf{R}_{\mathbf{N}_i\mathbf{N}_{i-1},z} = \begin{bmatrix} \cos\varepsilon_i & -\sin\varepsilon_i & 0 \\ \sin\varepsilon_i & \cos\varepsilon_i & 0 \\ 0 & 0 & 1 \end{bmatrix}, \tag{28a}$$

$$\mathbf{R}_{\mathbf{N}_i\mathbf{N}_{i-1},x}=\begin{bmatrix}1 & 0 & 0\\ 0 & \cos\varepsilon_i & -\sin\varepsilon_i\\ 0 & \sin\varepsilon_i & \cos\varepsilon_i\end{bmatrix}, \tag{28b}$$

$$\mathbf{R}_{\mathbf{N}_i\mathbf{N}_{i-1},y}=\begin{bmatrix}\cos\varepsilon_i & 0 & \sin\varepsilon_i\\ 0 & 1 & 0\\ -\sin\varepsilon_i & 0 & \cos\varepsilon_i\end{bmatrix}. \tag{28c}$$

In 2-D cases, Equation 28 can be simplified as

$$\mathbf{R}_{\mathbf{N}_i\mathbf{N}_{i-1}}=\begin{bmatrix}\cos\varepsilon_i & -\sin\varepsilon_i\\ \sin\varepsilon_i & \cos\varepsilon_i\end{bmatrix}. \tag{29}$$

5. Formulate deformation relations for node $\mathbf{N}_i$ as

$$\boldsymbol{\delta}_{\mathbf{N_i}}=\boldsymbol{\delta}_{\mathbf{N_{i-1}}}+\left[\prod_{j=1}^{i}\mathbf{R}_{\mathbf{N_jN_{j-1}}}\right]\left(\mathbf{N_i}-\mathbf{N_{i-1}}\right)-\left(\mathbf{N_i}-\mathbf{N_{i-1}}\right) \tag{30}$$

i.e.

$$\boldsymbol{\delta}_{\mathbf{N_i}}=\left\{\sum_{j=1}^{i}\left[\prod_{k=1}^{j}\mathbf{R}_{\mathbf{N_kN_{k-1}}}\right]\left(\mathbf{N_j}-\mathbf{N_{j-1}}\right)\right\}-\left(\mathbf{N_i}-\mathbf{N_0}\right). \tag{31}$$

6. After the deformation and tolerances of all nodes are obtained, find the total deformation and tolerance of assembly.

5 Case Study

A simple structure composed of two L-shaped structures, as shown in Figure 16, was studied to validate this approach. Its corresponding structural tree is shown in Figure 17.

Using Equation 29, the rotational matrices were formulated as follows:

$$\mathbf{R}_{\mathbf{AO}}=\begin{bmatrix}\cos\varepsilon_1 & -\sin\varepsilon_1\\ \sin\varepsilon_1 & \cos\varepsilon_1\end{bmatrix}$$

$$\mathbf{R}_{\mathbf{BA}} = \begin{bmatrix} \cos\varepsilon_2 & -\sin\varepsilon_2 \\ \sin\varepsilon_2 & \cos\varepsilon_2 \end{bmatrix}.$$

The deformation of **B** is derived according to Equation 31 as

$$\boldsymbol{\delta}_{\mathbf{B}} = \mathbf{R}_{\mathbf{AO}}(\mathbf{A}-\mathbf{O}) + \mathbf{R}_{\mathbf{BA}}\mathbf{R}_{\mathbf{AO}}(\mathbf{B}-\mathbf{A}) - \mathbf{B}.$$

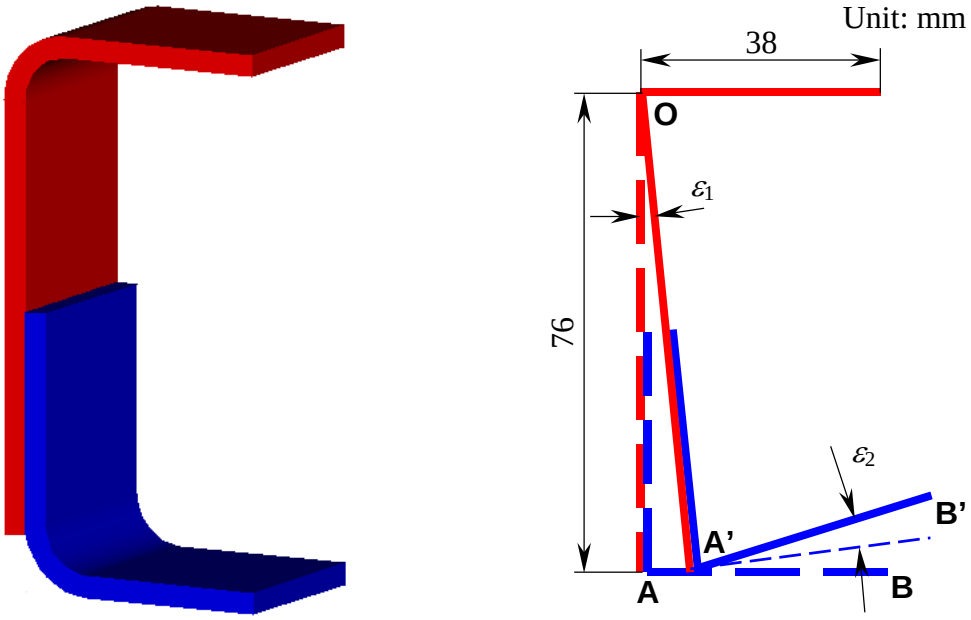

Figure 16: Assembly of two L-shaped structures

Figure 17: Structural tree for the assembly of two L-shaped structures

When E-glass/epoxy cross ply laminates were assumed and the fiber volume fraction is 49%, the displacement at **B** is

$$\boldsymbol{\delta}_{\mathbf{B}} = \begin{bmatrix} 76\sin\varepsilon_1 - 38[1-\cos(\varepsilon_1+\varepsilon_2)] \\ 76(1-\cos\varepsilon_1) + 38\sin(\varepsilon_1+\varepsilon_2) \end{bmatrix} = \begin{bmatrix} 0.48 \\ 0.48 \end{bmatrix}.$$

The total displacement at **B** is $\left\|\boldsymbol{\delta}_{\mathbf{B}}\right\|_2 = 0.68\,\text{mm}$. In order to verify the effectiveness of this method, the FEA analysis was also conducted. The displacement at **B** from the FEA, as shown in Figure 18, is 0.72 mm, which shows the STM can predict the assembly deformation of composites effectively and efficiently.

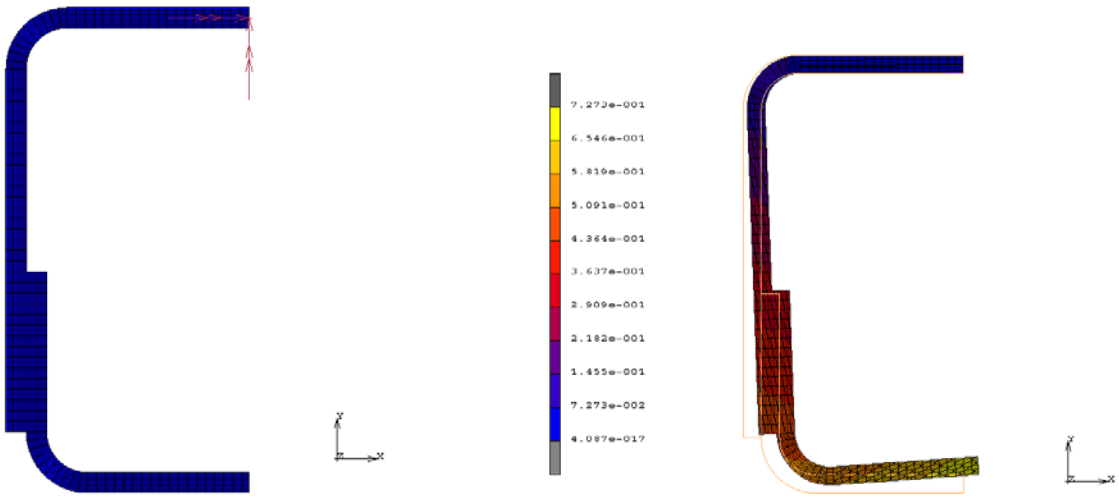

(a) Mesh (b) Deformation

Figure 18: FEA result for the assembly of two L-shaped structures

6 Conclusions

In this paper, an innovative dimension variation prediction method was developed. A dimension variation model was first developed for process simulation based on thermal stress analysis and finite element analysis (FEA). This model was validated against the analytical solutions, the data from open literature, and the experiments. The results show that although there are certain errors in some cases, this model can predict the dimension variations with adequate accuracy.

The regression-based dimension variation model was developed based on the typical structure study using the developed FEA-based dimension variation model. These typical structures include angled structures, single-stiffener structures, double-stiffener structures, cylindrical shells, hat shaped structures, structures with an open window, and 3-D stiffener structures were modeled. Data were collected by varying the design geometric parameters. Regression models were developed using the collected data. In order to make the non-linear regression models comprehensive, a material modification coefficient was introduced based on the analytical solution and FEA results. By incorporating this coefficient, the regression-based model can be applied to any fiber/resin type and/or any stacking sequence. The developed regression-based dimension variation model does not require FEA, thus it significantly reduces the amount of computation time and provides a quick guide for composite product design.

The structural tree method was developed to compute the deformation of general shape composite components and composite assemblies the regression-based dimension variation model. The advantage of this approach is that it does not need the finite element analysis, thus the amount of computation time is greatly reduced, which is crucial for practical applications. The methods presented in this paper provide a foundation to develop practical and proactive dimension control techniques.

References

[1] Mallick, P.K., *Fiber-Reinforced Composites: Materials, Manufacturing, and Design*, Marcel Dekker, Inc. (1993).

[2] Holmberg, J.A. and Berglund, L.A., "Manufacturing and Performance of RTM U-Beams," *Composites Part A*, 28A(6): 513-521 (1997).

[3] Albert, C. and Fernlund, G., "Spring-in and Warpage of Angled Composite Laminates," *Composite Science and Technology*, 62(14): 1895-1912 (2002).

[4] Radford, D.W. and Rennich, T.S., "Separating Sources of Manufacturing Distortion in Laminated Composites," *Journal of Reinforced Plastics and Composites*, 19(8): 621-641 (2000).

[5] Svanberg, J. M. and Holmberg, J. A., "An Experimental Investigation on Mechanisms for Manufacturing Induced Shape Distortions in Homogeneous and Balanced Laminates," *Composites Part A*, 32(6): 827-838 (2001).
[6] Jain, L.K. and Mai, Y.W., "On Residual Stress Induced Distortions during Fabrication of Composite Shells," *Proceedings of the 1995 10th Technical Conference of the American Society for Composites*, 261-270 (1995).
[7] Jain, L.K. and Mai, Y.W., "On Residual Stress Induced Distortions during Fabrication of Composite Shells," *Journal of Reinforced Plastics and Composites*, 15(8): 793-805 (1996).
[8] Jain, L.K. and Mai, Y.W., "Stresses and Deformations Induced during Manufacturing. Part I: Theoretical Analysis of Composite Cylinders and Shells," *Journal of Composite Materials*, 31(7) 673-695 (1997).
[9] Jain, L.K., Lutton, B.G., Mai, Y.W. and Paton, R., "Stresses and Deformations Induced during Manufacturing. Part II: A Study of the Spring-in Phenomenon," *Journal of Composite Materials*, 31(7) 696-719 (1997).
[10] Huang, C.K. and Yang, S.Y., "Warping in Advanced Composite Tools with Varying Angles and Radii," *Composites Part A*, 28A(9-10): 891-893 (1997).
[11] Meink, T. and Shen, M.H.H., "Processing Induced Warpage in Composite Cylindrical Shells Part I," *12th Engineering Mechanics Conference* (1998).
[12] Meink, T. and Shen, M.H.H., "Processing Induced Warpage in Composite Cylindrical Shells Part I," *ASME Winter Annual Meeting* (1998).
[13] Meink, T. and Shen, M.H.H., "Processing Induced Warpage in Composite Cylindrical Shells," in *Advances in composite materials and mechanics*, ed. by Arup Maji, American Society of Civil Engineers, Reston, VA, 1-12 (1999).
[14] Theriault, R. P., Osswald, T. A. and Castro, J.M., "Processing Induced Residual Stress in Asymmetric Laminate Panels," *Polymer Composites*, 20(3): 493-509 (1999).
[15] Wiersma, H.W., Peeters, L.J.B. and Akkerman, R., "Prediction of Springforward in Continuous-Fiber/Polymer L-Shaped Parts," *Composites Part A*, 29A(11): 1333-1342 (1998).
[16] Darrow, D.A., Jr. and Smith, L.V., "Evaluating the Spring-in Phenomenon of Polymer Matrix Composites," *33rd International SAMPE Technical Conference*, 33: 326-337 (2001).
[17] Darrow, D.A., Jr. and Smith, L.V., "Isolating Components of Processing Induced Warpage in Laminated Composites," *Journal of Composite Materials*, 36(21): 2407-2419 (2002).
[18] Golestanian, H. and El-Gizawy, A.S., "Modeling of Process Induced Residual Stresses in Resin Transfer Molded Composites with Woven Fiber Mats," *Journal of Composite Materials*, 35(1): 1513-1528 (2001).
[19] Wang, J., Kelly, D. and Hillier, W., "Finite Element Analysis of Temperature Induced Stresses and Deformations of Polymer Composite Components," *Journal of Composite Materials*, 34(17): 1456-1471 (2000).
[20] Fernlund, G., Nelson, K.M. and Poursartip, A., "Modeling of Process Induced Deformations of Composite Shell Structures," *45th International SAMPE Symposium and Exhibition*, 45(1): 169-177 (2000).
[21] Ding, Y., Chiu, W.K. and Liu, X.L., "Anisotropy Related 'Spring-in' of Angled Composite Shells," *Polymers & Polymer Composites*, 9(6): 393-401 (2001).

[22] Zhu, Q., Geubelle, P.H., Li, M. and Tucker, C.L., III, "Dimensional Accuracy of Thermoset Composites: Simulation of Process-Induced Residual Stresses," *Journal of Composite Materials*, 35(2): 2171-2205 (2001).
[23] Tsai, S.W. and Hahn, H.T., *Introduction to Composite Materials*, Technomic Pub. Co., Lancaster, PA (1980).
[24] Hall, D. and Clyne, T.W., *An Introduction to Composite Materials*, 2nd ed., Cambridge University Press, Cambridge, UK (1996).